IMEKO 23rd TC3, 13th TC5 and 4th TC22 International Conference
30 May to 1 June, 2017, Helsinki, Finland

COMPARISON OF EXPERIMENTAL AND THEORETICAL INDENTATION MODULI OF ANISOTROPIC SINGLE CRYSTALS

Yukimi Tanaka, Yutaka Seino, and Koichiro Hattori

National Metrology Institute of Japan, National Institute of Advanced Industrial Science and Technology (NMIJ-AIST), Tsukuba, Japan, yukimi.tanaka@aist.go.jp

Abstract: Nanoindentation is a useful method for measuring elastic modulus. However, the elastic modulus of anisotropic single crystal measured by nanoindentation is often different from theoretical value calculated by elastic constants. Hence, we investigated the cause of the problem above by measuring indentation moduli of 4H-SiC, sapphire and quartz with a Berkovich and a spherical indenter. Consequently, the experimental elastic moduli were 5-15 percent higher than the theoretical value regardless of indenter shape and calculation method. The difference between theoretical and experimental modulus suggests to be not concerned with underestimation of contact area due to plastic deformation such as pile-up.

Keywords: Nanoindentation, Elastic modulus, SiC, Sapphire, Quartz

1. INTRODUCTION

Nanoindentation is a useful method to evaluate regional elastic modulus. However, the elastic moduli of some single crystals measured by nanoindentation are often different from Young's moduli calculated by elastic constants. Especially, experimental elastic moduli of anisotropic materials like SiC and sapphire are higher than theoretical value [1-3]. However, the main cause of the difference is still incompletely understood. To clarify the cause of the difference, it is effective to evaluate elastic modulus during elastic deformation. In this study, the elastic moduli of anisotropic materials, 4H-SiC, sapphire and quartz, with a Berkovich indenter and a spherical indenter were compared with the theoretical value based on Delafargue-Ulm method [4]. For accurate evaluation in the nanoindentation experiments, two types of corrections, variable epsilon factor and gamma factor that corrects radial displacement, were applied. Additionally, we investigated the possible factors that were related to the difference between experimental and theoretical values.

2. THEORETICAL INDENTATION MODULUS

Oliver and Pharr [2,5] defined the relationship between unloading stiffness, S and indentation modulus, M of isotropic materials through the following equation:

$$S = \frac{2}{\sqrt{\pi}} M \sqrt{A} \qquad (1)$$

where A is the projected contact area. Moreover, Vlassak and Nix [6] indicated that Eq. (1) can be used for anisotropic materials. Delafargue and Ulm [4] proposed an explicit representation for the indentation moduli of a transversely isotropic material from elastic constants. The indentation modulus of perpendicular to isotropic plane, M_z can be calculated using the equation:

$$M_z = \sqrt{\frac{C_{11}C_{33} - C_{13}^2}{C_{11}}\left(\frac{1}{C_{44}} + \frac{2}{\sqrt{C_{11}C_{33}} + C_{13}}\right)^{-1}} \qquad (2)$$

The elastic constants of 4H-SiC, sapphire and quartz that were obtained from ultrasonic technique in previous research [7-9] were summarized in Table 1. In addition, indentation modulus of perpendicular to (0001) plane, M_z calculated from the elastic constants using Eq. (2) were shown in Table 1. Delafargue-Ulm method was applied to conical indenters. However, Vlassak and Nix have indicated that indentation moduli calculated from elastic constants for conical and spherical indenters were very close to each other [6]. Thus, the indentation moduli calculated from Delafargue-Ulm method were suggested to be nearly unchanged due to the difference of indenter geometry.

For isotropic materials, M is defined using Young's modulus, E and Poisson's ratio, v as, $M = E / (1 - v^2)$. However, this equitation cannot be applied to a general anisotropic material because of far more complexity than in

Table 1. Elastic constants, calculated theoretical indentation moduli and elastic moduli of various single crystals (GPa)

	C_{11}	C_{12}	C_{13}	C_{33}	C_{44}	M_z	v_{pt}	E_z
4H-SiC [7]	501	111	52	553	163	478	0.07	476
Sapphire [8]	497	164	111	498	147	433	0.16	422
Quartz [9]	87	7	12	106	58	108	0.11	107

the isotropic case [4,6]. In the case of transversely isotropic single crystals, Poisson's ratio was defined the ratio of perpendicular contraction strain to transverse extension strain and vice versa [10]. Since the indentation was on (0001) plane in our experiments, Poisson's ratio of perpendicular contraction to transverse extension, v_{pt} was calculated. Therefore, the theoretical elastic modulus of perpendicular to isotropic plane, E_z can be calculated using the equation:

$$E_z = \left(1 - v_{pt}^2\right) M_z \qquad (3)$$

as shown in Table 1.

3. METHODS

Nanoindentation-tests were carried out by using ENT-2100 (ELIONIX) with a Berkovich indenter and a 10 μm spherical indenter. The maximum loads were ranging 5-100 mN. Frame compliance was determined from compliance of sapphire because large stiff indentations could be obtained. With the Berkovich indenter, M_z was calculated by Oliver-Pharr method. On the other hand, with the spherical indenter, M_z was calculated by Hertzian contact method in addition to Oliver-Pharr method.

3.1. Oliver-Pharr method

The elastic moduli with Berkovich and spherical indenter were calculated using Oliver-Pharr method [2,5] with corrections of variable epsilon and radial displacement. First, stiffness $S = dP/dh$, defined as the slope of the unloading curve at the maximum depth. Then, contact depth h_c was determined from

$$h_c = h_{max} - \varepsilon \frac{P_{max}}{S} \qquad (4)$$

where h_{max} and P_{max} are the maximum of indentation depth and load respectively, and ε is the factor depending on indenter geometry. For Berkovich and spherical indenter, ε is usually used 0.75. However, this factor can be more accurate to be calculated from the power law exponents, m that is obtained by fitting to unloading curve. The epsilon factor was calculated using the equation [11]:

$$\varepsilon(m) = \frac{0.08158}{\sqrt{m - 0.94}} - \frac{0.61679}{(m - 0.94)^{0.02}} + \frac{1.26386}{(m - 0.94)^{0.001}} \qquad (5)$$

Area function for the Berkovich indenter and effective radius of the spherical indenter were determined by measuring Young's modulus of fused silica as reference material. Area function A for the Berkovich indenter was fitted with a truncated-tip approximation [12] as follows:

$$A(h_c) = C_0 (h_c + dh)^2 \qquad (6)$$

where C_0 and dh are fitting parameters. Owing to relatively large indentation depth in our experiments, the truncated-tip approximation was not so different from the polynomial approximation that Oliver-Pharr originally proposed. For spherical indenter, the area function was

$$A(h_c) = \pi\left(2 h_c R - h_c^2\right) \qquad (7)$$

where R is indenter radius obtained by fitting. Indentation modulus of perpendicular to isotropic plane, M_z was calculated from the following equation:

$$M_z = \frac{1}{\gamma} \frac{\sqrt{\pi}}{2} \frac{S}{\sqrt{A(h_c)}} \qquad (8)$$

where γ is a correction factor that depends on the shape of indenter [13,14]. The correction factor γ for Berkovich indenter [13] is

$$\gamma = \frac{\pi/4 + 0.15483073 \cot\phi \left((1 - 2v_{pt})/4(1 - v_{pt})\right)}{\left(\pi/2 - 0.83119312 \cot\phi \left((1 - 2v_{pt})/4(1 - v_{pt})\right)\right)^2} \qquad (9)$$

where ϕ is the half-included angle of the indenter. For spherical indenter [14] is

$$\gamma = 1 + \frac{2(1 - 2v_{pt})}{3\pi(1 - v_{pt})} \frac{a}{R} \qquad (10)$$

After obtaining M_z, experimental elastic modulus to isotropic plane E_z was calculated from the following equation:

$$E_z = \left(1 - v_{pt}^2\right) \left(\frac{1}{M_z} - \frac{1 - v_i^2}{E_i}\right)^{-1} \qquad (11)$$

where E_i is the elastic modulus of the indenter, and v_i is the Poisson's ratio of the indenter.

3.2. Hertzian contact method

Additionally, elastic modulus was also calculated from loading curve with analysis based on Hertzian contact method with the correction of radial displacement. Field and Swain [15] proposed that the stress-strain curves were obtained from indentation load, P and contact radius, a during the elastic deformation with spherical indenter. The relationship of the representative stress by $P/(\pi a^2)$ and representative strain by a/R is denoted by the following equation:

$$\frac{P}{\pi a^2} = \gamma \frac{4 M_z}{3\pi} \frac{a}{R} \qquad (12)$$

where γ is Eq. (10). The indentation modulus could be obtained by linear fitting to stress-strain curve in a range from 10 to h_{max} nm. When pop-in events occurred, the loading curve before the pop-in events was used to calculate indentation modulus. After obtaining M_z, elastic modulus to isotropic plane E_z was calculated using Eq. (11).

4. RESULT AND DISCUSSION

The load-displacement curves of 4H-SiC, sapphire and quartz under 100 mN loads with the Berkovich and the spherical indenter are shown in Fig. 1. The load-displacement curve indicated that the indentation with the

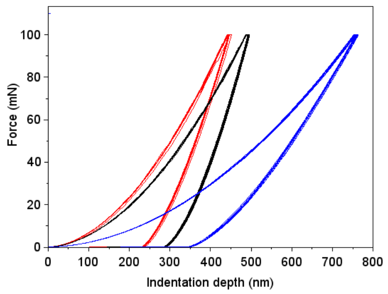

(a) Berkovich indenter

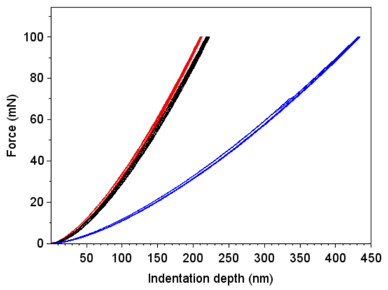

(b) Spherical indenter

Fig. 1. Load-displacement curve up to 100 mN with the Berkovich and the spherical indenter. Black, red and blue lines indicate sapphire, 4H-SiC and quartz, respectively.

spherical indenter is almost elastic deformation, whereas that with the Berkovich indenter is elasto-plastic deformation for all three materials. The small pop-in events were observed during the loading curve of quartz with the spherical indenter. Therefore, the elastic deformation of quartz with spherical indenter suggested to be before the pop-in event. The loading curve before the pop-in event were used to calculate elastic modulus by using Hertzian contact method.

The elastic moduli E_z of 4H-SiC, sapphire and quartz calculated by Oliver-Pharr method and Hertzian contact method with correction were shown in Fig. 2. The indentation moduli of all three material were higher than theoretical elastic moduli regardless of indenter shape and calculation method. In addition, the elastic moduli were nearly independent of indentation depth. Thus, it is suggested that the elastic modulus from indentation experiment is not varied with indentation depth, even if transversely isotropic materials are measured.

The average of experimental elastic moduli over 50 nm indentation depth were summarized in Table 2. The experimental elastic moduli became slightly closer to the theoretical value by applying correction. However, these moduli were still 5-15 percent higher than theoretical value. Therefore, the reason why the experimental elastic moduli was higher than theoretical values was not suggested to concern with these correction factor.

These results are suggested that the experimental elastic moduli during purely elastic deformation are almost the same as during elasto-plastic deformation. Therefore, the change of contact area such as pile-up has a small influence on the difference between experimental and theoretical elastic moduli. In addition, the elastic moduli were

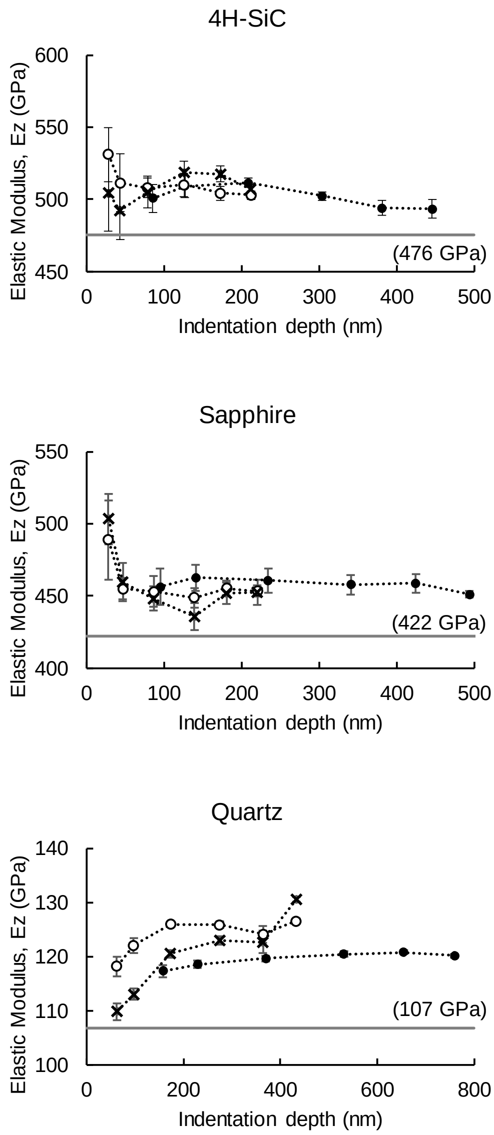

Fig. 2. The experimental elastic moduli of 4H-SiC, sapphire and quartz with correction. Error bar indicates the standard deviation of measurements. Filled circles: using Oliver-Pharr method with Berkovich indenter. Open circles: using Oliver-Pharr method with spherical indenter. Cross marks: using Hertzian contact theory with spherical indenter. Solid line: theoretical elastic moduli.

overestimated not only 4H-SiC and sapphire that have high elasticity but also quartz that has relatively low elasticity. Thus, the difference between experimental and theoretical values seem to be not caused by underestimating contact area or machine compliance depending on small indentation depth.

The experimental elastic moduli of transversely isotropic single crystals were different from the theoretical values even though the theoretical values were considered anisotropic. One possible reason is fused silica was used as reference material. Fused silica has amorphous structure, thus the deformation mechanism suggests to be different from single-crystals. The contact area that calculated from the measurement of fused silica may be not appropriate for measuring single crystals. Another possible reason is the

Table 2. Experimental elastic moduli of perpendicular to (0001) plane, E_z (h > 50 nm)

	4H-SiC		Sapphire		Quartz	
	E_Z (GPa)	E_Z (cor) (GPa)	E_Z (GPa)	E_Z (cor) (GPa)	E_Z (GPa)	E_Z (cor) (GPa)
Berkovich (O&P)	523 ± 10	502 ± 9	470 ± 9	458 ± 9	122 ± 1	119 ± 1
Spherical (O&P)	512 ± 6	506 ± 6	456 ± 7	453 ± 7	125 ± 3	124 ± 3
Spherical (Hertz)	518 ± 10	511 ± 9	451 ± 11	447 ± 11	121 ± 7	120 ± 7
Theoretical	476		422		107	

effect of anisotropy that is not considered in the present study. Since radial displacement correction that was proposed by Hay [13,14] were considered for isotropic materials, the elastic modulus of the direction parallel to isotropic plane was not taken into consideration. Radial displacement of anisotropic material is likely different from that of isotropic material. In addition to these possible reasons, there may be the errors of measuring displacement or load, friction of contact between indenter and sample surface, and the difference of indenter angle. To clarify further the difference between the experimental and theoretical modulus, it is needed to evaluate various materials such as cubic single crystals.

5. SUMMARY

In the present study, the elastic moduli of perpendicular to (0001) plane of 4H-SiC, sapphire and quartz with the Berkovich and the spherical indenter were compared with the theoretical elastic moduli. The experimental elastic moduli were 5-15 percent higher than the theoretical value regardless of indenter shape and calculation method. These results suggest that the difference between theoretical and experimental elastic modulus is not concerned with underestimation of contact area due to plastic deformation such as pile-up.

REFERENCES

[1] A. Datye, “Characterizing the mechanical behavior of single and polycrystalline silicon carbide using nanoindentation,” PhD Thesis, University of Tennessee, 2014.

[2] W.C. Oliver and G. M. Pharr, “An improved technique for determining hardness and elastic modulus using load and displacement sensing indentation experiments,” J. Mater. Res., vol. 7, pp. 1564-1483, 1992.

[3] C. Lu, Y. W. Mai, P. L. Tam and Y. G. Shen, “Nanoindentation-induced elastic-plastic transition and size effect in α-Al_2O_3(0001),” Phil. Mag. Lett., vol. 87, pp. 409-415, 2007.

[4] A. Delafargue and F. J. Ulm, “Explicit approximations of the indentation modulus of elastically orthotropic solids for conical indenters,” Int. J. Solid. Struct., vol. 41, pp. 7351-7360, 2004.

[5] W. C. Oliver and G. M. Pharr, “Measurement of hardness and elastic modulus by instrumented indentation: advances in understanding and refinements to methodology,” J. Mater. Res., vol. 19, pp. 3-20, 2004.

[6] J. J. Vlassak, M. Ciavarella, j. R. Barber and X. Wang, “The indentation modulus of elastically anisotropic materials for indenters of arbitrary shape,” J. Mech. Phys. Solid., vol. 51, pp. 1701-1721, 2003.

[7] K. Kamitani, M. Grimsditch, J. C. Nipko, C.-K. Loong, M. Okada and I. Kimura, “The elastic constants of silicon carbide: a Brillouin-scattering study of 4H and 6H SiC single crystals,” J. Appl. Phys., vol. 82, pp. 3152-3154, 1997.

[8] J. B. Wachtman, W. E. Tefft, D. G. Lam and R. P. Stinchfield, “Elastic constants of synthetic single crystal corundum at room temperature,” J. Res. Natl. Bur. Stand., vol. 64A, pp. 214-228, 1960.

[9] H. J. McSkimin, P. Andreatch Jr. and R. N. Thurston, “Elastic moduli of quartz versus hydrostatic pressure at 25 and -195.8 °C,” J. Appl. Phys., vol. 36, pp. 1624-1632, 1965.

[10] A. F. Bower, “Applied mechanics of solids,” CRC Press, chapter 3, 2009.

[11] ISO 14577-1 Metallic materials – Instrumented indentation test for hardness and materials parameters – Part1: Test method, 2015.

[12] A. Shimamoto, K. Tanaka, Y. Akiyama and Yoshizaki, “Nanoindentation of glass with a tip-truncated Berkovich indenter” Phil. Mag. A, vol. 7, pp. 1097-1105, 1994.

[13] J. C. Hay, A. Bolshakov and G. M. Pharr, “A critical examination of the fundamental relations used in the analysis of nanoindentation data,” J. Mater. Res., vol. 14, pp. 2296-2305, 1999.

[14] J. L. Hay and P. J. Wolff, “Small correction required when applying the Hertzian contact model to instrumented indentation data,” J. Mater. Res., vol. 16, pp. 1280-1286, 2001.

[15] J. S. Field and M. V. Swain, “The indentation characterisation of the mechanical properties of various carbon materials: glassy carbon, coke and pyrolytic graphite,” Carbon, vol. 34, pp. 1357-1366, 1996.